

## Article

# Discovery of Nine Dipeptidyl Peptidase-4 Inhibitors from *Coptis chinensis* Using Virtual Screening, Bioactivity Evaluation, and Binding Studies

Zixi Zhao <sup>1</sup>, Ruonan Ma <sup>1</sup>, Yuqing Ma <sup>1</sup>, Liqiang Zhao <sup>1</sup>, Lele Wang <sup>2</sup>, Yuzhen Fang <sup>2</sup>, Yuxin Zhang <sup>2,\*</sup>, Xia Wu <sup>1,\*</sup> and Xing Wang <sup>1,\*</sup> 

<sup>1</sup> School of Traditional Chinese Medicine, Capital Medical University, Fengtai District, Beijing 100069, China; zhaozixi@mail.ccmu.edu.cn (Z.Z.); maruonan@mail.ccmu.edu.cn (R.M.); mayuqing@mail.ccmu.edu.cn (Y.M.); zlq0615@mail.ccmu.edu.cn (L.Z.)

<sup>2</sup> School of Pharmacy, Minzu University of China, Haidian District, Beijing 100081, China; wanglele@muc.edu.cn (L.W.); fangyuzhen@muc.edu.cn (Y.F.)

\* Correspondence: zhangyuxin@muc.edu.cn (Y.Z.); wuxia6710@ccmu.edu.cn (X.W.); wangxing@ccmu.edu.cn (X.W.); Tel.: +86-10-83911633 (Xing Wang); Fax: +86-10-83911627 (Xing Wang)

**Abstract:** The objective of this study was to identify multiple alkaloids in *Coptis chinensis* that demonstrate inhibitory activity against DPP-4 and systematically evaluate their activity and binding characteristics. A combined strategy that included molecular docking, a DPP-4 inhibition assay, surface plasmon resonance (SPR), and a molecular dynamics simulation technique was employed. The results showed that nine alkaloids in *Coptis chinensis* directly inhibited DPP-4, with IC<sub>50</sub> values of 3.44–53.73 μM. SPR-based binding studies revealed that these alkaloids display rapid binding and dissociation characteristics when interacting with DPP-4, with K<sub>D</sub> values ranging from 8.11 to 29.97 μM. A molecular dynamics analysis revealed that equilibrium was rapidly reached by nine DPP-4–ligand systems with minimal fluctuations, while binding free energy calculations showed that the ΔG<sub>bind</sub> values for the nine test compounds ranged from −31.84 to −16.06 kcal/mol. The most important forces for the binding of these alkaloids with DPP-4 are electrostatic interactions and van der Waals forces. Various important amino acid residues, such as Arg125, His126, Phe357, Arg358, and Tyr547, were involved in the inhibition of DPP-4 by the compounds, revealing a mechanistic basis for the further optimization of these alkaloids as DPP-4 inhibitors. This study confirmed nine alkaloids as direct inhibitors of DPP-4 and characterized their binding features, thereby providing a basis for further research and development on novel DPP-4 inhibitors.

**Keywords:** natural DPP-4 inhibitors; *Coptis chinensis*; enzyme inhibitory activity; molecular dynamics; surface plasmon resonance



**Citation:** Zhao, Z.; Ma, R.; Ma, Y.; Zhao, L.; Wang, L.; Fang, Y.; Zhang, Y.; Wu, X.; Wang, X. Discovery of Nine Dipeptidyl Peptidase-4 Inhibitors from *Coptis chinensis* Using Virtual Screening, Bioactivity Evaluation, and Binding Studies. *Molecules* **2024**, *29*, 2304. <https://doi.org/10.3390/molecules29102304>

Academic Editors: Giovanni Lentini, Maria Maddalena Cavalluzzi and Solomon Habtemariam

Received: 7 April 2024  
Revised: 7 May 2024  
Accepted: 8 May 2024  
Published: 14 May 2024



**Copyright:** © 2024 by the authors. Licensee MDPI, Basel, Switzerland. This article is an open access article distributed under the terms and conditions of the Creative Commons Attribution (CC BY) license (<https://creativecommons.org/licenses/by/4.0/>).

## 1. Introduction

Dipeptidyl peptidase-4 (DPP-4) is an important target for the clinical treatment of several diseases including diabetes, obesity, cardiovascular diseases, and non-alcoholic fatty liver disease (NAFLD) [1–6]. As a serine protease on the surface of cells, DPP-4 plays a role in the breakdown of peptides, including incretin hormones such as glucagon-like peptide-1 (GLP-1) and glucose-dependent insulinotropic polypeptide (GIP) [7]. The inhibition of DPP-4 can prolong the half-lives of these peptides, leading to increased insulin secretion and improved glucose control. DPP-4 inhibitors have been developed as a class of antidiabetic drugs and are used in the treatment of type 2 diabetes [8]. By inhibiting DPP-4, these drugs can enhance the action of GLP-1 and GIP, resulting in better blood sugar control. DPP-4 inhibitors are generally well tolerated and have a low risk of hypoglycemia compared to other antidiabetic drugs. Overall, the clinical importance of DPP-4 as a target lies in its involvement in glucose homeostasis and the potential therapeutic applications

of DPP-4 inhibitors in diabetes and other related diseases. Therefore, inhibitors targeting DPP-4 have broad therapeutic potential for a variety of diseases.

At present, a variety of DPP-4 inhibitors, such as sitagliptin, vildagliptin, saxagliptin, alogliptin, linagliptin, gemigliptin, trelagliptin, and anagliptin, are marketed worldwide (Figure 1). These DPP-4 inhibitors have the advantages of definite hypoglycemic effects, a low risk of hypoglycemia, no weight gain, good cardiovascular safety, and once-daily administration [9–15]. However, some potential side effects are also associated with them, such as nasopharyngitis, headache, upper respiratory tract infection, and mild gastrointestinal discomfort. Some rare adverse reactions include acute pancreatitis, arthralgia, heart failure, angioneurotic edema, hypersensitivity, elevated liver enzymes, diarrhea, cough, and a decreased absolute lymphocyte count [16–21]. In addition, the dosage of some DPP-4 inhibitors needs to be adjusted according to renal function; the exception is linagliptin, which is mainly excreted through the intestine while the others are mainly excreted through the kidney [22–24].

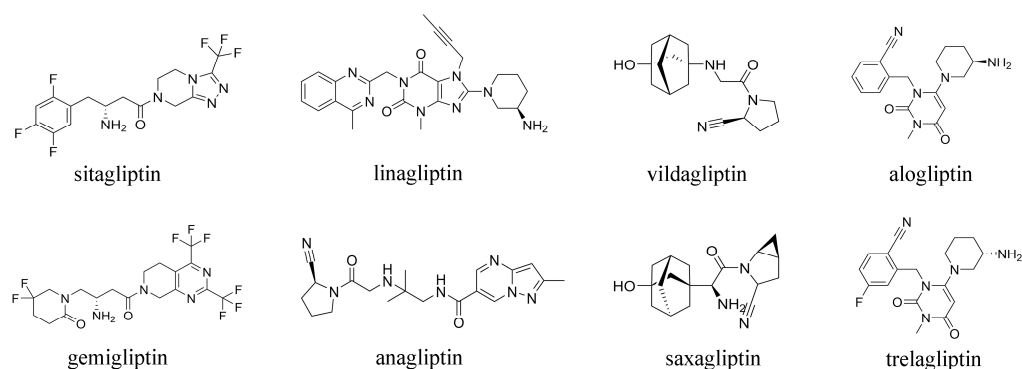


**Figure 1.** The structures of some DPP-4 inhibitors that are commercially available worldwide.

Compared with chemically synthesized drugs, natural herbal medicines are considered to have higher effectiveness and fewer side effects [25,26]. Therefore, an urgent need for novel DPP-4 inhibitors with good efficacy and safety in natural herbal medicines is recognized. *Coptis chinensis* is one of the earliest recognized and most valuable medicinal plants in China; it has been used to treat diabetes for over two thousand years. It has been shown to have various effects, such as lowering blood glucose, improving insulin secretion, and modulating intestinal microbiota [27–30]. Recent clinical studies have confirmed the efficacy of berberine (the main component of *Coptis chinensis*) for diabetes as it can induce insulin secretion in a glucose-dependent manner, thus avoiding the risk of hypoglycemia [31–33]. Therefore, it may be meaningful to screen and validate DPP-4 inhibitors from *Coptis chinensis* as they may offer new options for the development of effective and safe antidiabetic drugs.

This study accomplished the discovery and characterization of DPP-4 inhibitors from components of *Coptis chinensis* through an integrated approach that combined computational and experimental methods (Figure 2). Initially, molecular docking was performed to identify compounds with the potential to bind with DPP-4. Subsequently, an enzyme inhibition assay was used to validate the inhibitory activity of these potential compounds. Then, the SPR technique was employed to evaluate the affinity of the novel DPP-4 inhibitors for the DPP-4 protein and their binding–dissociation characteristics. Finally, a molecular dynamics simulation technique was used to analyze the interaction between the inhibitors and DPP-4. Natural DPP-4 inhibitors from *Coptis chinensis* were discovered in this work, which will facilitate the development of safe and effective DPP-4 inhibitors and reveal active ingredients in *Coptis chinensis* for treating diabetes.

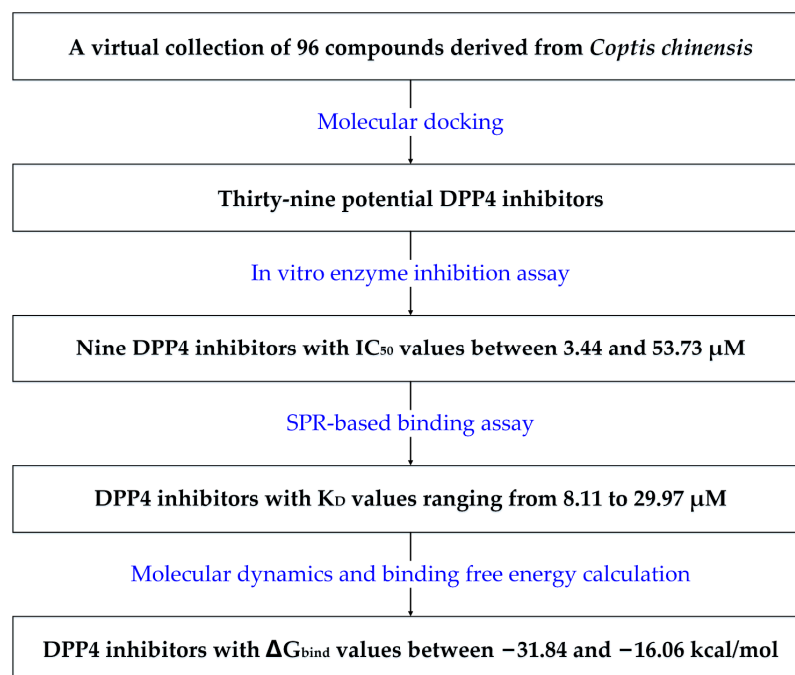


**Figure 2.** A schematic illustration of the discovery of DPP-4 inhibitors from *Coptis chinensis*.

## 2. Results

### 2.1. Potential DPP-4 Inhibitors Identified through Molecular Docking

The reliability of the docking program was confirmed by re-docking 8O3 into the active site of DPP-4 from the co-crystal structure. A total score of 6.25 was achieved for DPP-4-8O3, and an RMSD of 0.71 Å was observed between the co-crystallized and re-docked conformations of 8O3 (Figure 3). This suggests that the experimentally observed binding mode was accurately reproduced by the docking program as the docked conformation was highly similar to the co-crystallized conformation. The amino acids Arg125, Glu205, Glu206, Ser209, Tyr631, Tyr662, Tyr666, Asn710, and His740 played a critical role in inhibiting DPP-4 activity at the 8O3 binding site. A screening of 96 natural compounds for DPP-4 inhibitors was subsequently conducted using docking procedures, resulting in the identification of 39 hits with docking scores exceeding 6.00, which is the score for the re-docking of 8O3 with DPP-4, indicating that the compounds have a strong affinity for the target protein. Inhibitory activity against DPP-4 was then evaluated in vitro for these hits.

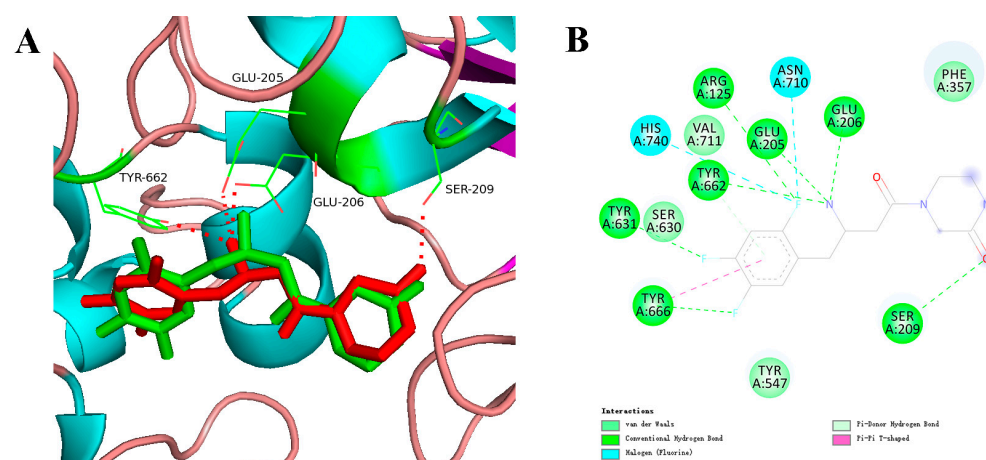


**Figure 3.** The interface (A) and interactions (B) between DPP-4 and ligand 8O3. Green and red sticks represent re-docked and co-crystallized conformations of 8O3, respectively. Red dotted lines indicate hydrogen bond interactions between ligands and DPP-4.

## 2.2. In Vitro Evaluation of DPP-4 Inhibitory Activity

In a primary screening, 40% DPP-4 inhibition was exhibited by nine alkaloids in *Coptis chinensis*, namely columbamine, demethyleneberberine, epiberberine, groenlandicine, coptisine, berberine, palmatine, jatrorrhizine, and berberrubine, at a final concentration of 30  $\mu$ M. Sitagliptin, which had an  $IC_{50}$  value of 0.41 nM (Figure 2.3), was used as a positive control. A further dose–response investigation revealed that nine alkaloids exhibited  $IC_{50}$  values of 3.44–53.73  $\mu$ M for DPP-4 inhibition (Figure 5). Columbamine had the strongest inhibitory activity, with an  $IC_{50}$  value of 3.44  $\mu$ M, while berberine had the weakest activity, with an  $IC_{50}$  value of 53.73  $\mu$ M.

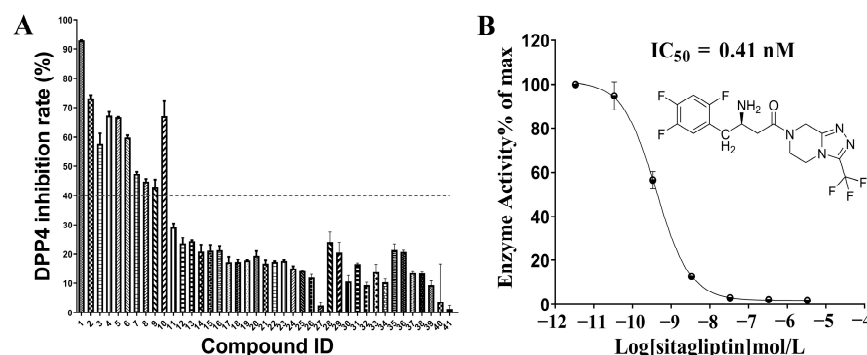


**Figure 4.** The initial screening results of the inhibitory activity of 39 compounds against DPP-4 (A) and the DPP-4 inhibitory activity of sitagliptin (B). In (A), the compounds represented by Compound IDs 1–40 are sitagliptin (CAS:486460-32-6), columbamine (CAS:3621-36-1), demethyleneberberine (CAS:25459-91-0), epiberberine (CAS:6873-09-2), groenlandicine (CAS:38691-95-1), coptisine (CAS:3486-66-6), berberine (CAS:2086-83-1), palmatine (CAS:3486-67-7), jatrorrhizine (CAS:3621-38-3), berberrubine (CAS:15401-69-1), ethyl caffeate (CAS:102-37-4), picrotin (CAS:21416-53-5), picroside ii (CAS:39012-20-9), protocatechuic acid methyl ester (CAS:2150-43-8), picroside i (CAS:27409-30-9), canadine (CAS:522-97-4), catalpol (CAS:2415-24-9), spongouridine (CAS:3083-77-0), caffeic acid dimethyl ether (CAS:2316-26-9), obacunone (CAS:751-03-1), isovanilline (CAS:621-59-0), D-mannoheptulose (CAS:3615-44-9), androsin (CAS:531-28-2), limonin (CAS:1180-71-8), N-trans-feruloyltyramine (CAS:66648-43-9), gentisic acid (CAS:490-79-9), danshensu (CAS:76822-21-4), sophocarpine (CAS:6483-15-4), sophoridine (CAS:6882-68-4), rhombifoline (CAS:529-78-2), N-methylcytisine (CAS:486-86-2), cytisine (CAS:485-35-8), D-tetrahydropalmatine (CAS:3520-14-7), phellodendrine (CAS:6873-13-8), corypalmine (CAS:27313-86-6), dauricine (CAS:524-17-4), sinomenine (CAS:115-53-7), phellodendrine chloride (CAS:104112-82-5), berbamine (CAS:478-61-5), and oxyberberine (CAS:549-21-3), respectively. The purity of all test compounds is above 98%, and the blank solvent is represented by compound ID 41. The DPP-4 inhibition rate (%) was calculated using the following formula: (maximum fluorescence value—sample fluorescence value)/maximum fluorescence value  $\times$  100%. The red dotted line indicates the 40% DPP4 inhibition rate line. In this study, compounds with a DPP4 inhibition rate higher than 40% were selected for further dose–response relationship analysis.

## 2.3. Interaction Analysis-Based Molecular Docking

Molecular docking was employed to investigate the binding sites between the ligands and DPP-4. The results showed that nine alkaloids had stable binding modes with DPP-4 (Figure 6). For instance, berberine formed two hydrogen bonds with the side chains of Ser630 and Arg669 and also established hydrophobic contacts with Glu205, Glu206, and Tyr666. Sitagliptin produced six hydrogen bonds with the side chains of Arg125, Glu205, Glu206, Ser209, and Ser552 and also had hydrophobic interactions with Tyr547 and Lys554. Some DPP-4 binding sites, including Glu205, Glu206, Tyr666, Phe357, and Arg125, can bind to at least four alkaloids, which may be a common characteristic of the interactions between these alkaloids and the DPP-4 protein. Some of the less frequently occurring amino acid residues, such as Arg358 for columbamine, Arg669 for berberine, and Lys554 and Tyr547 for sitagliptin, might be unique to the binding characteristics of these alkaloids.

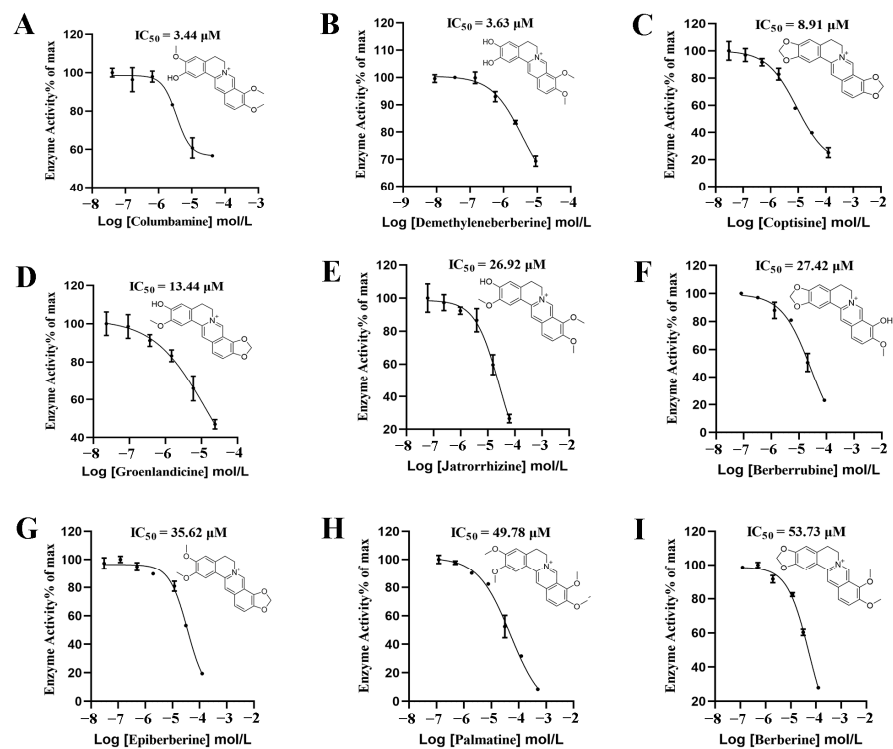


**Figure 5.** The DPP-4 inhibitory activity of columbamine (A), deMethyleneberberine (B), coptisine (C), groenlandicine (D), jatrorrhizine (E), berberrubine (F), epiberberine (G), palmatine (H), and berberine (I), measured using dose–response curves.

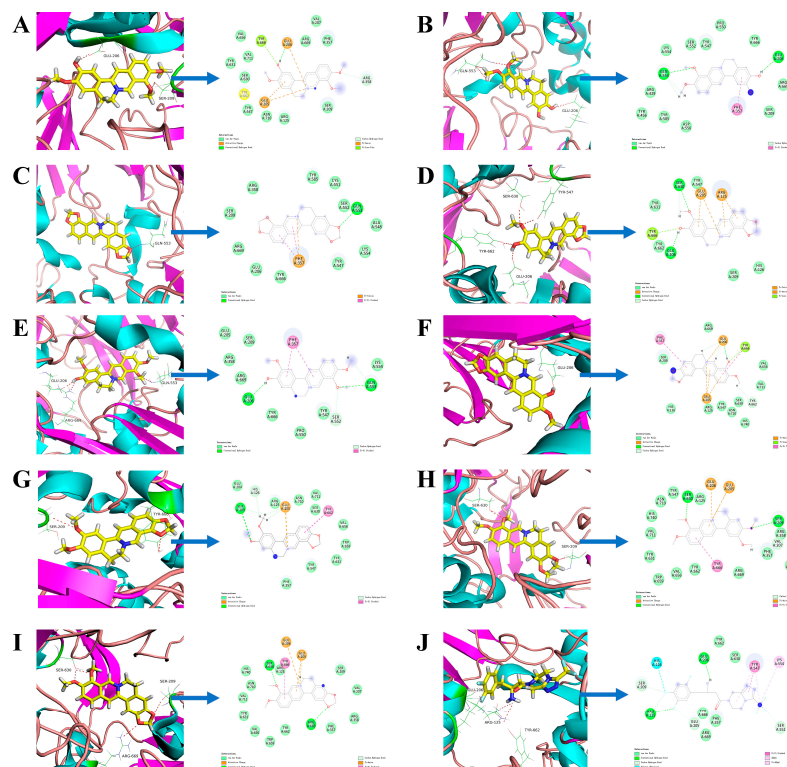


**Figure 6.** The interface of DPP-4 with various compounds including columbamine (A), deMethyleneberberine (B), coptisine (C), groenlandicine (D), Jatrorrhizine (E), berberrubine (F), epiberberine (G), palmatine (H), berberine (I), and sitagliptin (J) at the binding site.

## 2.4. Binding Analysis Based on SPR

An SPR-based binding study showed that the test alkaloids bound to DPP-4 with fast binding and fast dissociation characteristics, and they had varying affinities, with  $K_D$  values ranging from 8.11 to 29.97  $\mu\text{M}$  (Figure 7). The strongest affinity was observed for columbamine, with a  $K_D$  value of 8.11  $\mu\text{M}$ , while berberine exhibited a relatively weak affinity, with a  $K_D$  value of 29.97  $\mu\text{M}$ , which was consistent with the trend in its in vitro DPP-4 inhibitory activity.

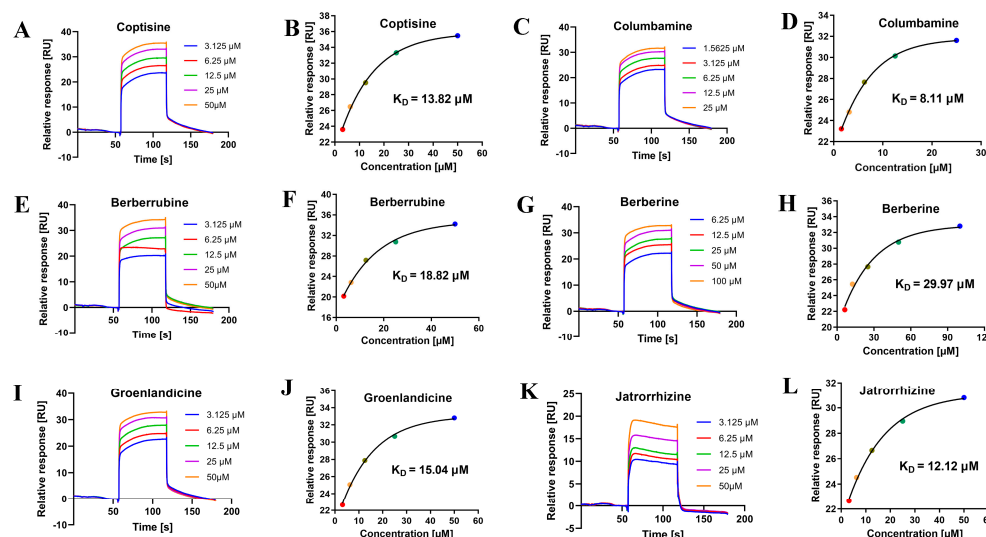


**Figure 7.** The sensorgrams and fitted curves for the binding and dissociation of DPP-4 with coptisine, columbamine, berberrubine, berberine, groenlandicine and jatrorrhizine (from (A) to (L)). The fitted curves were obtained using the ‘Affinity’ module of the evaluation software Biacore T200.

## 2.5. Molecular Dynamics Simulation

A molecular dynamics simulation was performed on the initial conformations of the DPP-4–inhibitor complexes obtained from the docking program. The RMSD values of the backbone atoms of DPP-4 relative to the initial structure were calculated to study the conformation dynamics of each system (Figure 8A). The results showed that the RMSD values of most compounds and DPP-4 complex system reached equilibrium quickly after 20 ns, with very low fluctuations (below 1 Å). However, coptisin and deMethyleneberberine reached equilibrium after 70 ns with very low fluctuations (below 1 Å). These results suggest that the protein conformation of DPP-4 could be bound and stabilized by the test compounds. Finally, the binding free energy and free energy decomposition of each system were calculated based on trajectory data from the last 20 ns.

The binding affinities of the nine DPP-4–ligand systems were calculated using MM/GBSA. The binding free energy ( $\Delta G_{\text{bind}}$ ) values for the nine test compounds ranged from  $-31.84$  to  $-16.06$  kcal/mol (Table 1). Hydrophobic, electrostatic, and hydrogen bonding interactions play important roles in the interactions between them. The hydrophobic groups of the nine alkaloids, which include multiple phenyl and methyl groups, interact with the hydrophobic region of the protein active pocket through amino acid residues such as Phe357, Tyr662, and Tyr666, thereby enhancing their affinity with the DPP-4 protein. Moreover, electrostatic interaction also plays a large role in the interaction between these nine alkaloids and DPP-4. The N atoms of the nine alkaloids, which are all quaternary ammonium alkaloids and carry positive charges, interact with a charged region in the protein active pocket, such as Glu205, Glu206, and other amino acid residues, increasing their affinity with the DPP-4 protein. The important structural basis for their DPP-4-inhibitory effect lies in the benzene ring, positively charged N atom, and hydroxyl group of these nine alkaloids, which enable them to bind firmly to DPP-4.

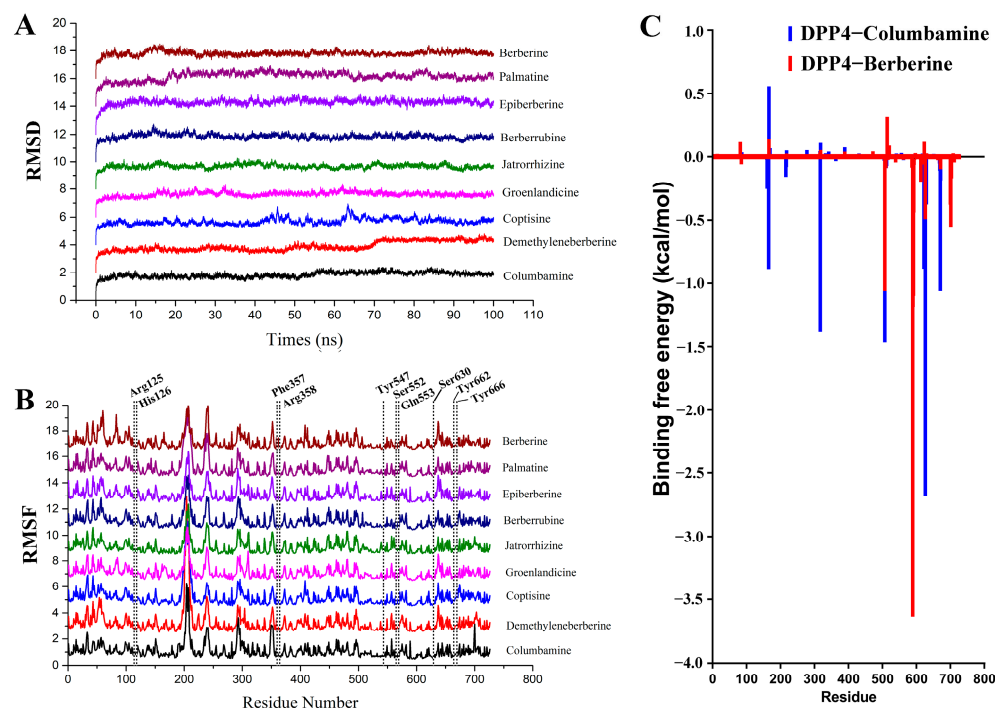


**Figure 8.** A molecular dynamics simulation analysis of DPP-4 and six of the test compounds. (A) The RMSD of the backbone atoms in the DPP-4–ligand system was calculated to evaluate the stability of the complex. The vertical offset was set to 2 in order to avoid overlap. (B) The RMSF values of the amino acid residues in the DPP-4–ligand system were computed to measure the flexibility of the protein. The key residues involved in binding are marked with dashed lines. The vertical offset was set to 2 in order to avoid overlap. (C) The MM/GBSA decomposition method was applied to estimate the contribution of each residue to the total binding free energies for the DPP-4–columbamine and DPP-4–berberine systems.

**Table 1.** Binding free energies and intermolecular interaction energy components of systems of DPP-4 and nine alkaloids in *Coptis chinensis*, calculated by the MM/GBSA approach (kcal/mol). Here, the van der Waals and coulomb energies are denoted by  $E_{vdw}$  and  $E_{ele}$ , respectively. The polar and non-polar solvation contributions,  $E_{GB}$  and  $E_{SURF}$ , were determined by solving the GB equations.  $G_{sol}$  represents the total solvation free energy, while  $G_{bind}$  represents the binding energy between DPP-4 and the ligands.  $G_{bind}$  was approximated by  $\Delta G_{bind} = G_{com} - (G_{pro} + G_{lig}) \approx \Delta E_{vdw} + \Delta E_{ele} + \Delta G_{sol}$ .

	Energy Component	Average	Std. Dev.	Std. Err. of Mean
DPP-4– Columbamine	$\Delta E_{vdw}$	−35.93	2.65	0.08
	$\Delta E_{ele}$	−282.02	8.30	0.26
	$\Delta E_{GB}$	291.16	7.77	0.25
	$\Delta E_{SURF}$	−5.05	0.16	0.00
	$\Delta G_{gas}$	−317.95	8.30	0.26
	$\Delta G_{sol}$	286.11	7.77	0.25
	$\Delta G_{bind}$	−31.84	2.54	0.08
DPP-4– Demethyleneberberine	$\Delta E_{vdw}$	−23.95	5.13	0.16
	$\Delta E_{ele}$	−277.99	17.25	0.55
	$\Delta E_{GB}$	276.92	16.17	0.51
	$\Delta E_{SURF}$	−3.70	0.41	0.01
	$\Delta G_{gas}$	−301.94	14.42	0.46
	$\Delta G_{sol}$	273.21	16.45	0.52
	$\Delta G_{bind}$	−28.73	5.45	0.17

Table 1. Cont.

	Energy Component	Average	Std. Dev.	Std. Err. of Mean
DPP-4- Coptisine	$\Delta E_{vdw}$	-28.79	2.24	0.07
	$\Delta E_{ele}$	-216.09	8.99	0.28
	$\Delta E_{GB}$	229.81	8.74	0.28
	$\Delta E_{SURF}$	-2.90	0.15	0.00
	$\Delta G_{gas}$	-244.88	9.13	0.29
	$\Delta G_{sol}$	226.91	8.70	0.28
	$\Delta G_{bind}$	-17.98	2.15	0.07
DPP-4- Groenlandicine	$\Delta E_{vdw}$	-23.60	3.52	0.11
	$\Delta E_{ele}$	-283.96	10.39	0.33
	$\Delta E_{GB}$	291.75	10.14	0.32
	$\Delta E_{SURF}$	-3.61	0.33	0.01
	$\Delta G_{gas}$	-307.57	11.24	0.36
	$\Delta G_{sol}$	288.15	9.98	0.32
	$\Delta G_{bind}$	-19.42	3.45	0.11
DPP-4- Jatrorrhizine	$\Delta E_{vdw}$	-32.43	2.76	0.09
	$\Delta E_{ele}$	-228.65	8.00	0.25
	$\Delta E_{GB}$	238.54	7.04	0.22
	$\Delta E_{SURF}$	-4.42	0.19	0.01
	$\Delta G_{gas}$	-261.09	8.05	0.25
	$\Delta G_{sol}$	234.11	7.03	0.22
	$\Delta G_{bind}$	-26.97	2.89	0.09
DPP-4- Berberrubine	$\Delta E_{vdw}$	-32.80	3.32	0.11
	$\Delta E_{ele}$	-289.40	10.88	0.34
	$\Delta E_{GB}$	300.01	8.61	0.27
	$\Delta E_{SURF}$	-4.55	0.23	0.01
	$\Delta G_{gas}$	-322.21	10.99	0.35
	$\Delta G_{sol}$	295.45	8.58	0.27
	$\Delta G_{bind}$	-26.75	4.77	0.15
DPP-4- Epiberberine	$\Delta E_{vdw}$	-30.50	2.68	0.08
	$\Delta E_{ele}$	-241.47	8.29	0.26
	$\Delta E_{GB}$	260.01	8.56	0.27
	$\Delta E_{SURF}$	-4.10	0.38	0.01
	$\Delta G_{gas}$	-271.98	9.41	0.30
	$\Delta G_{sol}$	255.92	8.38	0.26
	$\Delta G_{bind}$	-16.06	2.56	0.08
DPP-4- Palmatine	$\Delta E_{vdw}$	-33.91	2.33	0.07
	$\Delta E_{ele}$	-255.44	7.37	0.23
	$\Delta E_{GB}$	269.54	7.02	0.22
	$\Delta E_{SURF}$	-4.27	0.24	0.01
	$\Delta G_{gas}$	-289.35	7.45	0.24
	$\Delta G_{sol}$	265.27	6.98	0.22
	$\Delta G_{bind}$	-24.08	2.58	0.08
DPP-4- Berberine	$\Delta E_{vdw}$	-30.70	2.31	0.07
	$\Delta E_{ele}$	-204.52	12.53	0.40
	$\Delta E_{GB}$	218.71	12.96	0.41
	$\Delta E_{SURF}$	-3.20	0.36	0.01
	$\Delta G_{gas}$	-235.23	12.68	0.40
	$\Delta G_{sol}$	215.51	12.82	0.41
	$\Delta G_{bind}$	-19.72	2.40	0.08

The root mean square fluctuation (RMSF) of each amino acid residue of the DPP-4 protein was calculated to investigate the binding stability of the nine test compounds with DPP-4 (Figure 8B). A similar RMSF distribution was observed for the nine systems overall. Lower RMSF values were exhibited by the key common amino acid residues (i.e., Arg125, His126, Phe357, Arg358, Tyr547, Ser552, Gln553, Ser630, Tyr662, and Tyr666) than the other

regions of DPP-4, which means that a strong binding force was exerted by them toward DPP-4 and the tested compounds.

### 3. Discussion

Although previous studies in the literature reported that berberine, the main component of *Coptis chinensis*, demonstrates inhibitory activity against DPP-4, this study found that several other alkaloids in *Coptis chinensis* in addition to berberine can also inhibit DPP-4's activity, and some of them demonstrate stronger activity than berberine. This discovery possesses innovative value and provides references for revealing the relationship between the DPP-4 inhibitory activity of isoquinoline alkaloids and their structures, providing new clues for the development of more effective DPP-4 inhibitors.

In the enzymatic reaction assay, the IC<sub>50</sub> values of berberine were found to be close to those reported in the literature [34,35], and the other eight alkaloids all demonstrated stronger DPP-4 inhibitory activity than berberine. Using columbine and berberine as examples, the structures and activities of the alkaloids in *Coptis chinensis* were analyzed. Columbine has a hydroxyl and methoxy group at the same position as the methanedioxy group of berberine, which allows columbine to form hydrogen bonds and hydrophobic interactions with the key amino acid residues (e.g., Glu206 and Tyr666) of the DPP-4 protein. These interactions enhance the binding affinity of columbine with the DPP-4 protein. Similar observations were made for demethyleneberberine, berberrubine, and jatrorrhizine. This phenomenon was confirmed by both SPR-based binding assays and molecular dynamics simulations. Columbamine has a stronger affinity and a lower binding free energy than berberine, indicating that the hydroxyl group on the isoquinoline core can enhance the affinity between alkaloids and DPP-4 protein, thereby improving its DPP-4 inhibitory activity (Table S1).

The material basis and mechanism of the use of *Coptis chinensis* in diabetes treatment are further expanded in this work. In addition to berberine, many kinds of alkaloids in *Coptis chinensis* also possess DPP-4 inhibitory activity, which suggests that *Coptis chinensis*'s hypoglycemic effect may be the result of the collective action of its various alkaloids. Numerous studies have reported that many alkaloids, including palmatine, columbamine, and coptisine, possess properties such as reducing blood sugar, promoting insulin secretion, improving insulin resistance, and enhancing glucose utilization [36–41]. A comprehensive improvement in streptozotocin-induced diabetic mice was observed when various alkaloids in *Coptis chinensis* were combined, as evidenced by lowered blood sugar levels, an increased insulin content, and an improved lipid metabolism [42]. A theoretical basis for the application of *Coptis chinensis* in the treatment of diabetes is provided by these findings. Although all these alkaloids have the ability to inhibit DPP-4, their differing chemical structures and binding characteristics suggest a potential synergistic role in diabetes treatment. The combination of these alkaloids in a drug formulation has the potential to enhance clinical efficacy and reduce adverse reactions and drug resistance, thereby offering new insights and directions for the development of diabetes drugs.

## 4. Materials and Methods

### 4.1. Molecular Docking-Based Virtual Screening

To identify DPP-4 inhibitors in *Coptis chinensis*, a virtual library of 96 compounds from *Coptis chinensis* was constructed for a docking-based virtual screening using Surflex-Dock, a semi-flexible docking program, in the Sybyl X-2.0 package (Tripos, Cincinnati, OH, USA). Surflex-Dock employs a unique empirical scoring function and a search engine based on molecular similarity to dock ligand molecules to protein binding sites. The compound library was downloaded from the NCBI PubChem database (<https://www.ncbi.nlm.nih.gov/pccompound>, accessed on 16 January 2024.) in 2D (sdf) format. The optimization of these compounds and the molecular docking process were carried out according to our previous work [43,44].

The target protein for docking is the A chain of the DPP-4 crystal structure (PDB ID: 5Y7H), which was resolved by X-ray crystallography at 3.00 Å resolution [45]. The preparation of the DPP-4 crystal structure involved the elimination of crystallographic water molecules and the addition of hydrogen atoms. Subsequently, an energy minimization process was conducted utilizing an AMBER7 F99 force field. This process was carried out in accordance with the standard parameters of the SYBYL X-2.0 software. The DPP-4 active site, located within the binding pocket, is defined as the area within a 0.5 Å distance from the recognized inhibitor 8O3, chemically known as (R)-4-(3-amino-4-(2,4,5-trifluorophenyl)butanoyl)piperazin-2-one, with the molecular formula C<sub>14</sub>H<sub>16</sub>F<sub>3</sub>N<sub>3</sub>O<sub>2</sub> [45].

In order to evaluate the precision and robustness of the docking program, 8O3 was removed from the co-crystal structure and subsequently re-docked into the DPP-4 active site using the pre-established parameters of the Surflex-Dock docking program. The root mean square deviation (RMSD) was employed to measure the discrepancy between the co-crystallized and docked configurations of all heavy atoms in 8O3, as dictated by the subsequent formula [46]: “d” represents the distance between N pairs of corresponding atoms, with hydrogen atoms being the exception. A smaller RMSD value indicates a greater similarity between the co-crystal and docked configurations of 8O3. Diagrams of the protein–ligand contacts were generated using the show 2D Diagram program in Discovery Studio 3.0 software.

$$\text{RMSD} = \sqrt{\frac{1}{N} \sum_{i=1}^{i=N} d_i^2}$$

#### 4.2. DPP-4 Inhibition Assay

The DPP-4 inhibitory activity of 39 potential compounds obtained via virtual screening was tested using a commercial DPP-4 inhibitor screening assay kit (Item No. 700210, Cayman Chemical Company, Ann Arbor, MI, USA), and the kit’s instructions were followed exactly. The fluorescence intensity was measured at an excitation/emission wavelength of 360/460 nm using an EnVision Multilabel Reader (2104 PerkinElmer, Waltham, MA, USA). The possibility of false positives was eliminated by assessing the autofluorescence of each test compound. The test compounds, documented to be isolated from *Coptis chinensis* and structurally identified [47–50], were purchased from MCE (Medchem Express, Monmouth Junction, NJ, USA) and had a purity exceeding 98% (Figures S1–S18). These compounds were prepared at a concentration of 30 µM in deionized water that contained 0.5% DMSO. Sitagliptin (0.60 µM, Sigma-Aldrich, St. Louis, MO, USA) was used as a positive control, while deionized water containing 0.5% DMSO served as a negative control [51]. The half-maximal inhibitory concentration (IC<sub>50</sub>) was determined using GraphPad Prism 9 software.

#### 4.3. SPR-Based Binding Assay

The binding affinity between DPP-4 and six alkaloids in *Coptis chinensis* was evaluated using the BIAcore T200 system (GE Healthcare, Uppsala, Sweden). All SPR-related materials were obtained from GE Healthcare, and DPP-4 (D3446) was purchased from Sigma-Aldrich Chemical Co. (St. Louis, MO, USA). The DPP-4 protein, dissolved in PBS at a concentration of 40 ng/µL, was immobilized onto the surface of a CM5 sensor chip using a standard amine-coupling procedure. The test compounds were prepared at varying concentrations in a solution of Tris-HCl (pH 8.0) and injected over the surface of the chip at a rate of 30 µL·min<sup>−1</sup> and a temperature of 25 °C. A reference flow cell without the immobilization of DPP-4 served as a control for non-specific binding. The association and dissociation kinetics of each test compound with DPP-4 were observed for a duration of 1 min. The chip could be regenerated and reused multiple times after it was treated with glycine-HCl (10 mM; pH 2.0). The test compounds were evaluated using the single-cycle kinetics mode across a two-fold concentration series (1.17–100 µM). The equilibrium con-

stant ( $K_D$ ) was calculated based on the 1:1 reaction ratio between the molecule and protein, using the ‘affinity’ module in the Biacore T200 software [52].

#### 4.4. Molecular Dynamics and Binding Free Energy Calculation

A molecular dynamics simulation was applied to analyze the binding features and free energy of nine alkaloids in *Coptis chinensis* with the DPP-4 protein. A simulation system was set up which included a combination of the DPP-4 protein, a test compound, ions, and water, according to our previous work [43]. The initial atomic coordinates of the DPP-4-inhibitor complex were obtained using the Surflex-Dock method for the molecular dynamics simulation. Nine separate simulation boxes were created to enable the molecular dynamics simulation of nine compounds binding to DPP-4.

The geometry of the ligand was optimized using the B3LYP/6-31G\* level of theory, while the formal charges were computed using the HF/6-31G\* method in the program Gaussian 09 [53]. Partial charges were generated by fitting the electrostatic potentials with the Gaussian program, employing the restrained electrostatic potential (RESP) fitting technique found in the Amber20 package [54]. Each system’s water box was constructed with the TIP3P water model [55], and either chlorine or sodium ions were introduced to achieve system neutrality prior to the MD simulation. The DPP-4 protein and the ligands were assigned the ff14SB force field and the general Amber force field (GAFF), respectively, utilizing the LEaP module in the Amber20 package [56].

To achieve a low-energy starting conformation for the subsequent MD simulations, energy minimization was performed on each simulation box. Initially, the steepest descent method was employed with four thousand steps, followed by the conjugate gradient method with six thousand steps. The minimization process was carried out on the entire simulation system, which included the protein, ligand, ions, and water. Subsequently, the solutes, which consisted of the protein and ligand, were minimized. The system was heated from 0 to 300 K over a period of 300 ps using a Langevin thermostat system under a canonical ensemble and a harmonic restraint force constant set at  $10.0 \text{ kcal mol}^{-1} \text{ \AA}^{-2}$ . The system was equilibrated for a duration of 10 ns under conditions of constant temperature and pressure (isothermal–isobaric), maintaining a pressure of 1.0 bar. The barostat bath’s relaxation time was established at 2.0 ps. Following this, the production simulation was carried out for 100 ns under isothermal–isobaric conditions, with periodic boundary conditions in place. A time step of 2 fs was chosen, and the SHAKE algorithm was utilized to constrain the bonds involving hydrogen atoms. The particle mesh Ewald method was employed to manage long-range electrostatic interactions [57]. For short-range interactions, a cut-off value of 10.0 Å was set.

The binding free energy for DPP-4 and each test compound was estimated using molecular mechanics energies and techniques such as generalized born and surface area continuum solvation [58]. The total binding free energy was further dissected into individual contributions from each amino acid residue, facilitating the identification of the most crucial residues in the binding of DPP-4 to each test compound using the MM/GBSA decomposition method [59].

#### 4.5. Statistical Method

Statistical analysis and graphical representation were carried out using GraphPad Prism V9 software (GraphPad Software, San Diego, CA, USA). Data obtained from in vitro experiments were subjected to an ANOVA (one-way analysis of variance) and Dunnett’s multiple comparison test for analysis. A \*\*\**p* value of less than 0.001 was considered significant.

## 5. Conclusions

Nine alkaloids from *Coptis chinensis* were discovered to be direct DPP-4 inhibitors were discovered from by employing a systematic strategy of computational simulation, biological verification, and binding studies. The anti-DPP-4 activity and binding characteristics of these compounds were evaluated using multiple methods. The characteristics of the

binding between DPP-4 and the nine alkaloids present a valuable reference for future research to enhance their efficacy and selectivity via structural optimization, thereby laying the foundation for the development of DPP-4-targeting agents. Moreover, this study forms a basis and reference for understanding the material basis and mechanism underlying the therapeutic effect of *Coptis chinensis* on diabetes.

**Supplementary Materials:** The following supporting information can be downloaded at <https://www.mdpi.com/article/10.3390/molecules29102304/s1>, Figures S1–S18: The <sup>1</sup>H NMR spectra and HPLC chromatograms of columbamine, demethyleneberberine, epiberberine, groenlandicine, coptisine, berberine, palmatine, jatrorrhizine, and berberrubine. Table S1. Summary of the information of the DPP-4 inhibitors discovered in this study.

**Author Contributions:** Conceptualization, X.W. (Xing Wang), X.W. (Xia Wu) and Y.Z.; methodology, Z.Z., R.M. and X.W. (Xing Wang); software, Y.M.; validation, R.M., L.Z. and L.W.; formal analysis, Y.F.; investigation, X.W. (Xing Wang), X.W. (Xia Wu) and Y.Z.; resources, X.W. (Xing Wang); data curation, L.W., L.Z. and Y.F.; writing—original draft preparation, X.W. (Xing Wang) and Z.Z.; writing—review and editing, X.W. (Xia Wu); visualization, Y.M.; supervision, X.W. (Xing Wang), X.W. (Xia Wu) and Y.Z.; project administration, X.W. (Xing Wang); funding acquisition, X.W. (Xing Wang). All authors have read and agreed to the published version of the manuscript.

**Funding:** This research was funded by the National Natural Science Foundation of China (grant numbers 82374112 and 82204644) and the Project of the Scientific Research Ability Improvement Plan (grant number 2023QNTS44) at Minzu University of China.

**Institutional Review Board Statement:** Not applicable.

**Informed Consent Statement:** Not applicable.

**Data Availability Statement:** Data are contained within the article.

**Acknowledgments:** We thank Yuhong Xiang from Capital Normal University and Meiyong Fu from the Hainan Academy of Agricultural Sciences for their support with computing services.

**Conflicts of Interest:** The authors declare no conflicts of interest.

## References

1. Niebrzydowska-Tatus, M.; Pelech, A.; Bien, K.; Mekler, J.; Santiago, M.; Kimber-Trojnar, Z.; Trojnar, M. Association of dpp-4 concentrations with the occurrence of gestational diabetes mellitus and excessive gestational weight gain. *Int. J. Mol. Sci.* **2024**, *25*, 1829. [[CrossRef](#)] [[PubMed](#)]
2. D'Andrea, E.; Wexler, D.J.; Kim, S.C.; Paik, J.M.; Alt, E.; Patorno, E. Comparing effectiveness and safety of sglT2 inhibitors vs dpp-4 inhibitors in patients with type 2 diabetes and varying baseline hba1c levels. *JAMA Intern. Med.* **2023**, *183*, 242–254. [[CrossRef](#)] [[PubMed](#)]
3. Wang, K.; Zhang, Z.; Hang, J.; Liu, J.; Guo, F.; Ding, Y.; Li, M.; Nie, Q.; Lin, J.; Zhuo, Y.; et al. Microbial-host-isozyme analyses reveal microbial dpp4 as a potential antidiabetic target. *Science* **2023**, *381*, eadd5787. [[CrossRef](#)] [[PubMed](#)]
4. Zhuge, F.; Ni, Y.; Nagashimada, M.; Nagata, N.; Xu, L.; Mukaida, N.; Kaneko, S.; Ota, T. Dpp-4 inhibition by linagliptin attenuates obesity-related inflammation and insulin resistance by regulating m1/m2 macrophage polarization. *Diabetes* **2016**, *65*, 2966–2979. [[CrossRef](#)] [[PubMed](#)]
5. Pham, T.K.; Nguyen, T.; Yi, J.M.; Kim, G.S.; Yun, H.R.; Kim, H.K.; Won, J.C. Evogliptin, a dpp-4 inhibitor, prevents diabetic cardiomyopathy by alleviating cardiac lipotoxicity in db/db mice. *Exp. Mol. Med.* **2023**, *55*, 767–778. [[CrossRef](#)] [[PubMed](#)]
6. Oh, J.H.; Jun, D.W.; Kim, H.Y.; Lee, S.M.; Yoon, E.L.; Hwang, J.; Park, J.H.; Lee, H.; Kim, W.; Kim, H. Discovery of dipeptidyl peptidase-4 inhibitor specific biomarker in non-alcoholic fatty liver disease mouse models using modified basket trial. *Clin. Mol. Hepatol.* **2022**, *28*, 497–509. [[CrossRef](#)] [[PubMed](#)]
7. Stensen, S.; Gasbjerg, L.S.; Rosenkilde, M.M.; Vilsboll, T.; Holst, J.J.; Hartmann, B.; Christensen, M.B.; Knop, F.K. Endogenous glucose-dependent insulinotropic polypeptide contributes to sitagliptin-mediated improvement in beta-cell function in patients with type 2 diabetes. *Diabetes* **2022**, *71*, 2209–2221. [[CrossRef](#)] [[PubMed](#)]
8. Almaghthali, A.G.; Alkhalidi, E.H.; Alzahrani, A.S.; Alghamdi, A.K.; Alghamdi, W.Y.; Kabel, A.M. Dipeptidyl peptidase-4 inhibitors: Anti-diabetic drugs with potential effects on cancer. *Diabetes Metab. Syndr.-Clin. Res. Rev.* **2019**, *13*, 36–39. [[CrossRef](#)] [[PubMed](#)]
9. Lyseng-Williamson, K.A. Sitagliptin. *Drugs* **2007**, *67*, 587–597. [[CrossRef](#)]
10. Henness, S.; Keam, S.J. Vildagliptin. *Drugs* **2006**, *66*, 1989–2001, 2002–2004. [[CrossRef](#)]
11. Garnock-Jones, K.P. Saxagliptin/dapagliflozin: A review in type 2 diabetes mellitus. *Drugs* **2017**, *77*, 319–330. [[CrossRef](#)] [[PubMed](#)]

12. Keating, G.M. Alogliptin: A review of its use in patients with type 2 diabetes mellitus. *Drugs* **2015**, *75*, 777–796. [[CrossRef](#)] [[PubMed](#)]
13. Laffel, L.M.; Danne, T.; Klingensmith, G.J.; Tamborlane, W.V.; Willi, S.; Zeitler, P.; Neubacher, D.; Marquard, J. Efficacy and safety of the sglT2 inhibitor empagliflozin versus placebo and the dpp-4 inhibitor linagliptin versus placebo in young people with type 2 diabetes (dinamo): A multicentre, randomised, double-blind, parallel group, phase 3 trial. *Lancet Diabetes Endocrinol.* **2023**, *11*, 169–181. [[CrossRef](#)] [[PubMed](#)]
14. Song, Y.; Yang, H.; Kim, J.; Lee, Y.; Kim, S.H.; Do, I.G.; Park, C.Y. Gemigliptin, a dpp4 inhibitor, ameliorates nonalcoholic steatohepatitis through amp-activated protein kinase-independent and ulk1-mediated autophagy. *Mol. Metab.* **2023**, *78*, 101806. [[CrossRef](#)] [[PubMed](#)]
15. Liu, Z.; Xu, L.; Xing, M.; Xu, X.; Wei, J.; Wang, J.; Kang, W. Trelagliptin succinate: Dpp-4 inhibitor to improve insulin resistance in adipocytes. *Biomed. Pharmacother.* **2020**, *125*, 109952. [[CrossRef](#)]
16. Wu, M.Z.; Chandramouli, C.; Wong, P.F.; Chan, Y.H.; Li, H.L.; Yu, S.Y.; Tse, Y.K.; Ren, Q.W.; Yu, S.Y.; Tse, H.F.; et al. Risk of sepsis and pneumonia in patients initiated on sglT2 inhibitors and dpp-4 inhibitors. *Diabetes Metab.* **2022**, *48*, 101367. [[CrossRef](#)] [[PubMed](#)]
17. Fralick, M.; Colacci, M.; Thiruchelvam, D.; Gomes, T.; Redelmeier, D.A. Sodium-glucose co-transporter-2 inhibitors versus dipeptidyl peptidase-4 inhibitors and the risk of heart failure: A nationwide cohort study of older adults with diabetes mellitus. *Diabetes Obes. Metab.* **2021**, *23*, 950–960. [[CrossRef](#)]
18. Zannad, F.; Rossignol, P. Dipeptidyl peptidase-4 inhibitors and the risk of heart failure. *Circulation* **2019**, *139*, 362–365. [[CrossRef](#)]
19. Lepelley, M.; Khouri, C.; Lacroix, C.; Bouillet, L. Angiotensin-converting enzyme and dipeptidyl peptidase-4 inhibitor-induced angioedema: A disproportionality analysis of the who pharmacovigilance database. *J. Allergy Clin. Immunol.* **2020**, *8*, 2406–2408. [[CrossRef](#)]
20. Ohyama, K.; Shindo, J.; Takahashi, T.; Takeuchi, H.; Hori, Y. Pharmacovigilance study of the association between dipeptidyl peptidase-4 inhibitors and angioedema using the fda adverse event reporting system (faers). *Sci. Rep.* **2022**, *12*, 13122. [[CrossRef](#)]
21. Kim, N.H.; Choi, J.; Kim, N.H.; Choi, K.M.; Baik, S.H.; Lee, J.; Kim, S.G. Dipeptidyl peptidase-4 inhibitor use and risk of diabetic retinopathy: A population-based study. *Diabetes Metab.* **2018**, *44*, 361–367. [[CrossRef](#)]
22. Ceriello, A.; De Nigris, V.; Iijima, H.; Matsui, T.; Gouda, M. The unique pharmacological and pharmacokinetic profile of teneligliptin: Implications for clinical practice. *Drugs* **2019**, *79*, 733–750. [[CrossRef](#)] [[PubMed](#)]
23. Golightly, L.K.; Drayna, C.C.; Mcdermott, M.T. Comparative clinical pharmacokinetics of dipeptidyl peptidase-4 inhibitors. *Clin. Pharmacokinet.* **2012**, *51*, 501–514. [[CrossRef](#)] [[PubMed](#)]
24. Fuchs, H.; Runge, F.; Held, H.D. Excretion of the dipeptidyl peptidase-4 inhibitor linagliptin in rats is primarily by biliary excretion and p-gp-mediated efflux. *Eur. J. Pharm. Sci.* **2012**, *45*, 533–538. [[CrossRef](#)] [[PubMed](#)]
25. Wang, J.; Ma, Q.; Li, Y.; Li, P.; Wang, M.; Wang, T.; Wang, C.; Wang, T.; Zhao, B. Research progress on traditional chinese medicine syndromes of diabetes mellitus. *Biomed. Pharmacother.* **2020**, *121*, 109565. [[CrossRef](#)] [[PubMed](#)]
26. Tian, J.; Jin, D.; Bao, Q.; Ding, Q.; Zhang, H.; Gao, Z.; Song, J.; Lian, F.; Tong, X. Evidence and potential mechanisms of traditional chinese medicine for the treatment of type 2 diabetes: A systematic review and meta-analysis. *Diabetes Obes. Metab.* **2019**, *21*, 1801–1816. [[CrossRef](#)]
27. Lyu, Y.; Lin, L.; Xie, Y.; Li, D.; Xiao, M.; Zhang, Y.; Cheung, S.; Shaw, P.C.; Yang, X.; Chan, P.; et al. Blood-glucose-lowering effect of coptidis rhizoma extracts from different origins via gut microbiota modulation in db/db mice. *Front. Pharmacol.* **2021**, *12*, 684358. [[CrossRef](#)] [[PubMed](#)]
28. Ran, Q.; Wang, J.; Wang, L.; Zeng, H.R.; Yang, X.B.; Huang, Q.W. Rhizoma coptidis as a potential treatment agent for type 2 diabetes mellitus and the underlying mechanisms: A review. *Front. Pharmacol.* **2019**, *10*, 805. [[CrossRef](#)]
29. Huang, W.Y.; Dong, H. Coptidis rhizoma-contained traditional formulae for insomnia: A potential to prevent diabetes? *Chin. J. Integr. Med.* **2018**, *24*, 785–788. [[CrossRef](#)]
30. Xiao, S.; Liu, C.; Chen, M.; Zou, J.; Zhang, Z.; Cui, X.; Jiang, S.; Shang, E.; Qian, D.; Duan, J. Scutellariae radix and coptidis rhizoma ameliorate glycolipid metabolism of type 2 diabetic rats by modulating gut microbiota and its metabolites. *Appl. Microbiol. Biotechnol.* **2020**, *104*, 303–317. [[CrossRef](#)]
31. Zhang, Y.; Gu, Y.; Ren, H.; Wang, S.; Zhong, H.; Zhao, X.; Ma, J.; Gu, X.; Xue, Y.; Huang, S.; et al. Gut microbiome-related effects of berberine and probiotics on type 2 diabetes (the premote study). *Nat. Commun.* **2020**, *11*, 5015. [[CrossRef](#)] [[PubMed](#)]
32. Wang, S.; Ren, H.; Zhong, H.; Zhao, X.; Li, C.; Ma, J.; Gu, X.; Xue, Y.; Huang, S.; Yang, J.; et al. Combined berberine and probiotic treatment as an effective regimen for improving postprandial hyperlipidemia in type 2 diabetes patients: A double blinded placebo controlled randomized study. *Gut Microbes* **2022**, *14*, 2003176. [[CrossRef](#)] [[PubMed](#)]
33. He, Q.; Dong, H.; Guo, Y.; Gong, M.; Xia, Q.; Lu, F.; Wang, D. Multi-target regulation of intestinal microbiota by berberine to improve type 2 diabetes mellitus. *Front. Endocrinol.* **2022**, *13*, 1074348. [[CrossRef](#)]
34. Naik, S.; Deora, N.; Pal, S.K.; Ahmed, M.Z.; Alqahtani, A.S.; Shukla, P.K.; Venkatraman, K.; Kumar, S. Purification, biochemical characterization, and dpp-iv and alpha-amylase inhibitory activity of berberine from *cardiospermum halicacabum*. *J. Mol. Recognit.* **2022**, *35*, e2983. [[CrossRef](#)] [[PubMed](#)]
35. Al-Masri, I.M.; Mohammad, M.K.; Tahaa, M.O. Inhibition of dipeptidyl peptidase iv (dpp iv) is one of the mechanisms explaining the hypoglycemic effect of berberine. *J. Enzym. Inhib. Med. Chem.* **2009**, *24*, 1061–1066. [[CrossRef](#)] [[PubMed](#)]

36. Ma, H.; He, K.; Zhu, J.; Li, X.; Ye, X. The anti-hyperglycemia effects of rhizoma coptidis alkaloids: A systematic review of modern pharmacological studies of the traditional herbal medicine. *Fitoterapia* **2019**, *134*, 210–220. [[CrossRef](#)]
37. Wang, K.; Feng, X.; Chai, L.; Cao, S.; Qiu, F. The metabolism of berberine and its contribution to the pharmacological effects. *Drug Metab. Rev.* **2017**, *49*, 139–157. [[CrossRef](#)] [[PubMed](#)]
38. Shi, L.L.; Jia, W.H.; Zhang, L.; Xu, C.Y.; Chen, X.; Yin, L.; Wang, N.Q.; Fang, L.H.; Qiang, G.F.; Yang, X.Y.; et al. Glucose consumption assay discovers coptisine with beneficial effect on diabetic mice. *Eur. J. Pharmacol.* **2019**, *859*, 172523. [[CrossRef](#)]
39. Yang, T.C.; Chao, H.F.; Shi, L.S.; Chang, T.C.; Lin, H.C.; Chang, W.L. Alkaloids from coptis chinensis root promote glucose uptake in c2c12 myotubes. *Fitoterapia* **2014**, *93*, 239–244. [[CrossRef](#)]
40. Tian, X.; Zhang, Y.; Li, H.; Li, Y.; Wang, N.; Zhang, W.; Ma, B. Palmatine ameliorates high fat diet induced impaired glucose tolerance. *Biol. Res.* **2020**, *53*, 39. [[CrossRef](#)]
41. Ekeuku, S.O.; Pang, K.L.; Chin, K.Y. Palmatine as an agent against metabolic syndrome and its related complications: A review. *Drug Des. Dev. Ther.* **2020**, *14*, 4963–4974. [[CrossRef](#)] [[PubMed](#)]
42. Ma, B.; Tong, J.; Zhou, G.; Mo, Q.; He, J.; Wang, Y. Coptis chinensis inflorescence ameliorates hyperglycaemia in 3t3-l1 preadipocyte and streptozotocin-induced diabetic mice. *J. Funct. Food.* **2016**, *21*, 455–462. [[CrossRef](#)]
43. Li, Y.; Zhang, Y.; Wu, X.; Gao, Y.; Guo, J.; Tian, Y.; Lin, Z.; Wang, X. Discovery of natural 15-*l*-ox small molecule inhibitors from chinese herbal medicine using virtual screening, biological evaluation and molecular dynamics studies. *Bioorganic Chem.* **2021**, *115*, 105197. [[CrossRef](#)] [[PubMed](#)]
44. Wang, X.; Zhang, Y.; Liu, Q.; Ai, Z.; Zhang, Y.; Xiang, Y.; Qiao, Y. Discovery of dual eta/etb receptor antagonists from traditional chinese herbs through in silico and in vitro screening. *Int. J. Mol. Sci.* **2016**, *17*, 389. [[CrossRef](#)] [[PubMed](#)]
45. Lee, H.K.; Kim, M.K.; Kim, H.D.; Kim, H.J.; Kim, J.W.; Lee, J.O.; Kim, C.W.; Kim, E.E. Unique binding mode of evogliptin with human dipeptidyl peptidase iv. *Biochem. Biophys. Res. Commun.* **2017**, *494*, 452–459. [[CrossRef](#)] [[PubMed](#)]
46. Wang, X.; Guo, J.; Ning, Z.; Wu, X. Discovery of a natural syk inhibitor from chinese medicine through a docking-based virtual screening and biological assay study. *Molecules* **2018**, *23*, 3114. [[CrossRef](#)] [[PubMed](#)]
47. Liang, X.G.; Wu, F.; Wang, Y.J.; Fu, Z.; Wang, Y.; Feng, Y.; Liang, S. Research on bitter components from coptis chinensis based on electronic tongue. *Zhongguo Zhong Yao Za Zhi* **2014**, *39*, 3326–3329. [[PubMed](#)]
48. Zhong, F.; Shen, C.; Qi, L.; Ma, Y. A multi-level strategy based on metabolic and molecular genetic approaches for the characterization of different coptis medicines using hplc-uv and rad-seq techniques. *Molecules* **2018**, *23*, 3090. [[CrossRef](#)] [[PubMed](#)]
49. Long, C.Y.; Yang, Y.; Huang, S.X.; Zhang, L.; Yang, Y.; Guo, Y.L. Changing regularity of alkaloids from coptis chinensis before and after processing based on hr-ms-database. *Chin. Tradit. Herb. Drugs* **2018**, *53*, 5972–5979.
50. Qi, L.; Ma, Y.; Zhong, F.; Shen, C. Comprehensive quality assessment for rhizoma coptidis based on quantitative and qualitative metabolic profiles using high performance liquid chromatography, fourier transform near-infrared and fourier transform mid-infrared combined with multivariate statistical analysis. *J. Pharm. Biomed. Anal.* **2018**, *161*, 436–443. [[CrossRef](#)]
51. Krishna, R.; Herman, G.; Wagner, J.A. Accelerating drug development using biomarkers: A case study with sitagliptin, a novel dpp4 inhibitor for type 2 diabetes. *Aaps J.* **2008**, *10*, 401–409. [[CrossRef](#)] [[PubMed](#)]
52. Schnapp, G.; Klein, T.; Hoevels, Y.; Bakker, R.A.; Nar, H. Comparative analysis of binding kinetics and thermodynamics of dipeptidyl peptidase-4 inhibitors and their relationship to structure. *J. Med. Chem.* **2016**, *59*, 7466–7477. [[CrossRef](#)] [[PubMed](#)]
53. Frisch, M.J.; Trucks, G.W.; Schlegel, H.B.; Scuseria, G.E.; Robb, M.A.; Cheeseman, J.R.; Scalmani, G.; Barone, V.; Petersson, G.A.; Nakatsuji, H. *Gaussian-16 Revision c. 01 (2016)*; Gaussian Inc.: Wallingford, CT, USA, 2016.
54. Case, D.A.; Belfon, K.; Ben-Shalom, I.; Brozell, S.R.; Cerutti, D.; Cheatham, T.; Cruzeiro, V.W.D.; Darden, T.; Duke, R.E.; Giambasu, G. Amber 2020. 2020. Available online: <https://ambermd.org/CiteAmber.php> (accessed on 16 January 2024).
55. Pathak, A.K.; Bandyopadhyay, T. Temperature induced dynamical transition of biomolecules in polarizable and nonpolarizable tip3p water. *J. Chem. Theory Comput.* **2019**, *15*, 2706–2718. [[CrossRef](#)] [[PubMed](#)]
56. Song, D.; Wang, W.; Ye, W.; Ji, D.; Luo, R.; Chen, H.F. Ff14idps force field improving the conformation sampling of intrinsically disordered proteins. *Chem. Biol. Drug Des.* **2017**, *89*, 5–15. [[CrossRef](#)] [[PubMed](#)]
57. Harris, J.A.; Liu, R.; Martins, D.O.V.; Vazquez-Montelongo, E.A.; Henderson, J.A.; Shen, J. Gpu-accelerated all-atom particle-mesh ewald continuous constant ph molecular dynamics in amber. *J. Chem. Theory Comput.* **2022**, *18*, 7510–7527. [[CrossRef](#)]
58. Genheden, S.; Ryde, U. Comparison of end-point continuum-solvation methods for the calculation of protein-ligand binding free energies. *Proteins* **2012**, *80*, 1326–1342. [[CrossRef](#)]
59. Wu, F.; Hou, X.; Luo, H.; Zhou, M.; Zhang, W.; Ding, Z. Exploring the selectivity of pi3k $\alpha$  and mtor inhibitors by 3d-qsar, molecular dynamics simulations and mm/gbsa binding free energy decomposition. *Medchemcomm* **2013**, *4*, 1482. [[CrossRef](#)]

**Disclaimer/Publisher’s Note:** The statements, opinions and data contained in all publications are solely those of the individual author(s) and contributor(s) and not of MDPI and/or the editor(s). MDPI and/or the editor(s) disclaim responsibility for any injury to people or property resulting from any ideas, methods, instructions or products referred to in the content.